The Alignment of a Voltage-Sensing Peptide in Dodecylphosphocholine Micelles and in Oriented Lipid Bilayers by Nuclear Magnetic Resonance and Molecular Modeling

Kimmo Mattila, Rudolf Kinder, and Burkhard Bechinger
Max-Planck-Institut für-Biochemie, 82152 Martinsried, Germany

ABSTRACT The S4 segments of voltage-gated sodium channels are important parts of the voltage-sensing elements of these proteins. Furthermore, the addition of the isolated S4 polypeptide to planar lipid bilayers results in stepwise increases of ion conductivity. In order to gain insight into the mechanisms of pore formation by amphipathic peptides, the structure and orientation of the S4 segment of the first internal repeat of the rat brain II sodium channel was investigated in the presence of DPC micelles by multidimensional solution NMR spectroscopy and solid-state NMR spectroscopy on oriented phospholipid bilayers. Both the anisotropic chemical shift observed by proton-decoupled ^{15}N solid-state NMR spectroscopy and the attenuating effects of DOXYL-stearates on TOCSY crosspeak intensities of micelle-associated S4 indicate that the central α-helical portion of this peptide is oriented approximately parallel to the membrane surface. Simulated annealing and molecular dynamics calculations of the peptide in a biphasic tetrachloromethane-water environment indicate that the peptide α-helix extends over ~12 residues. A less regular structure further toward the C-terminus allows for the hydrophobic residues of this part of the peptide to be positioned in the tetrachloromethane environment. The implications for possible pore-forming mechanisms are discussed.

INTRODUCTION

Voltage-dependent sodium, potassium, and calcium channels are members of the same superfamily of proteins. Primary sequence comparison and biochemical analysis indicate that the α-subunit of the sodium channels and the α_1-subunit of the calcium channels contain four homologous domains arranged in tandem repeats (e.g., Fig. 1 in Betz, 1990; also reviewed in Montal, 1990; Stühmer, 1991; Sigworth, 1992). Each domain of voltage-gated channels is composed of five apolar and one amphipathic segment (S4), all of which have been suggested to cross the membrane. The S4 segments are composed of hydrophobic and several conserved basic residues at every third position. The accumulation of charged residues (Noda et al. 1984), mutagenesis (e.g., Stühmer et al., 1989; Logothetis et al., 1992; Chen et al., 1996; Kontis et al., 1997), and fluorescence labeling experiments (Mannuzzu et al., 1996) suggest that the S4 segments form a critical part of the voltage-sensing elements. Transmembrane voltage-induced conformational changes involving the S4 segments have, therefore, been suggested to result in the observed opening of the channel when the membrane is depolarized, or its deactivation upon hyperpolarization (Kra-Oz et al., 1992; Yang et al., 1996; Kontis et al., 1997).

Large channel proteins have been fragmented and the resulting domains investigated to reveal structure-function relationships (Oblatt-Montal et al., 1993; Doak et al., 1996; Ben-Efraim and Shai, 1996; Wray et al., 1999). Furthermore, the investigation of pore-forming model peptides has improved our understanding of the structure and function of antibiotic compounds (Bechinger, 1996; Vogt and Bechinger, 1999). Synthetic peptides with the amino acid sequence of S4 of the sodium channels produce voltage-dependent cation-selective channels in planar lipid bilayers (Tosteson et al., 1989; Brullemans et al., 1994). Voltage-dependent pore formation has also been observed for model peptides with reduced amino acid heterogeneity, but a similar distribution of charges (Iwata et al., 1994). S4 causes frequent and well-defined stepwise conductivity increases in addition to continuously active openings (Tosteson et al., 1989). These latter events should, therefore, correlate with low-energy configurations also observed by structural methods. In contrast, the stochastic channel openings observed with other amphipathic peptides, such as cecropins or magainins, are rare events and difficult to reproduce (Bechinger, 1997b). These sequences also carry high positive charge densities.

Received for publication 5 April 1999 and in final form 12 July 1999.

Address reprint requests to Dr. Burkhard Bechinger, Max-Planck-Institute for Biochemistry, Am Klopferspitz 18A, 82152 Martinsried, Germany. Tel.: +49-89-8578-2466; Fax: +49-89-8578-2876; E-mail: bechinge@biochem.mpg.de.

Kimmo Mattila's present address is Center for Scientific Computing (CSC), Tietotie 6, 02100 Espoo, Finland. E-mail: Kimmo.Mattila@csc.fi.

Abbreviations used: CD, circular dichroism; CVFF, consistent valence force field; DMF, *N,N*-dimethylformamide; DOPC, 1,2-dioleoyl-*sn*-glycero-3-phosphocholine; DPC, dodecylphosphocholine; EDT, 1,2-ethanedithiol; FTIR, Fourier-transform infrared; HBTU, *O*-(benzotriazol-1-yl)-1,1,3,3-tetramethyluronium hexafluorophosphate; HMP, *p*-hydroxymethylphonoxymethyl polysterene; HOBt, 1-hydroxybenzotriazol; HPLC, high-performance liquid chromatography; MD, molecular dynamics; NMP, *N*-methylpyrrolidone; NMR, nuclear magnetic resonance; NOESY, nuclear Overhauser effect spectroscopy; NVE, microcanonical ensemble; POPC, 1-palmitoyl-2-oleoyl-*sn*-glycero-3-phosphocholine; POPS, 1-palmitoyl-2-oleoyl-*sn*-glycero-3-phosphoserine; SA, simulated annealing; t-Bu, tertiary butyl; TFE, trifluoroethanol; TFA, trifluoro acetic acid; TOCSY, total correlation spectroscopy.

0006-3495/99/10/2102/12 $2.00

CD, FTIR, and NMR spectroscopies show a high helical content of the S4 fragment of the sodium channel as well as their derivatives in the presence of lipid bilayers or membrane-mimetic environments (Mulvey et al., 1989; Haris et al., 1994; Iwata et al., 1994; Brullemans et al., 1994; Doak et al., 1996). NMR spectroscopic investigations indicate that in organic solvents the α-helix of the S4 peptide of domain I of the rat brain sodium channel extends from residues 2 to 14 (Mulvey et al., 1989). In the presence of DPC micelles the helical portion of the peptide is slightly shifted toward the C-terminus (Doak et al., 1996; this study). The resulting lengths of the helices (15–20 Å) are, therefore, too short to span the hydrophobic core of a lipid bilayer completely ($\geq$30 Å).

Helical wheel analysis of the central region of various S4 peptides indicates that the α-helical conformation of S4 results in an amphipathic distribution of residues with one face consisting solely of hydrophobic amino acids (Fig. 1 *A*). The opposite face is composed of mostly polar and charged residues, with some hydrophobic residues being interspersed in-between. A 3_{10} helical conformation has also been suggested for S4 (Fig. 1 *B*), as such a conformation results in a higher hydrophobic moment and a cleaner amphipathic separation of hydrophobic and charged residues (Iwata et al., 1994). In order to understand the formation of voltage-gated pores by S4 peptides, further investigations of the interactions of this peptide with lipid bilayers are necessary.

We therefore studied the alignment of the S4 peptide in oriented lipid bilayers by proton-decoupled ^{15}N solid-state NMR spectroscopy. In addition, the structure, topology, and membrane penetration of S4 were investigated by solution NMR spectroscopy in the presence of detergent micelles which have been doped with spin-labeled fatty acids. These solid-state and solution NMR structural studies were complemented by molecular modeling and MD simulations in a hydrophobic/hydrophilic interface. Other amphipathic peptides that have been modeled in lipid bilayers or in membrane-mimetic environments include melittin (Berneche et al., 1998), alamethicin (Biggin et al., 1997), viral channel peptides (Grice et al., 1997), magainins (Milik and Skolnick, 1993; Ducarme et al., 1998), or a fragment of the human parathyroid hormone receptor (Pellegrini et al., 1998). Also in this study, molecular modeling and MD calculations agree well with the experimental data, even though they are performed in a simplified system (Guba and

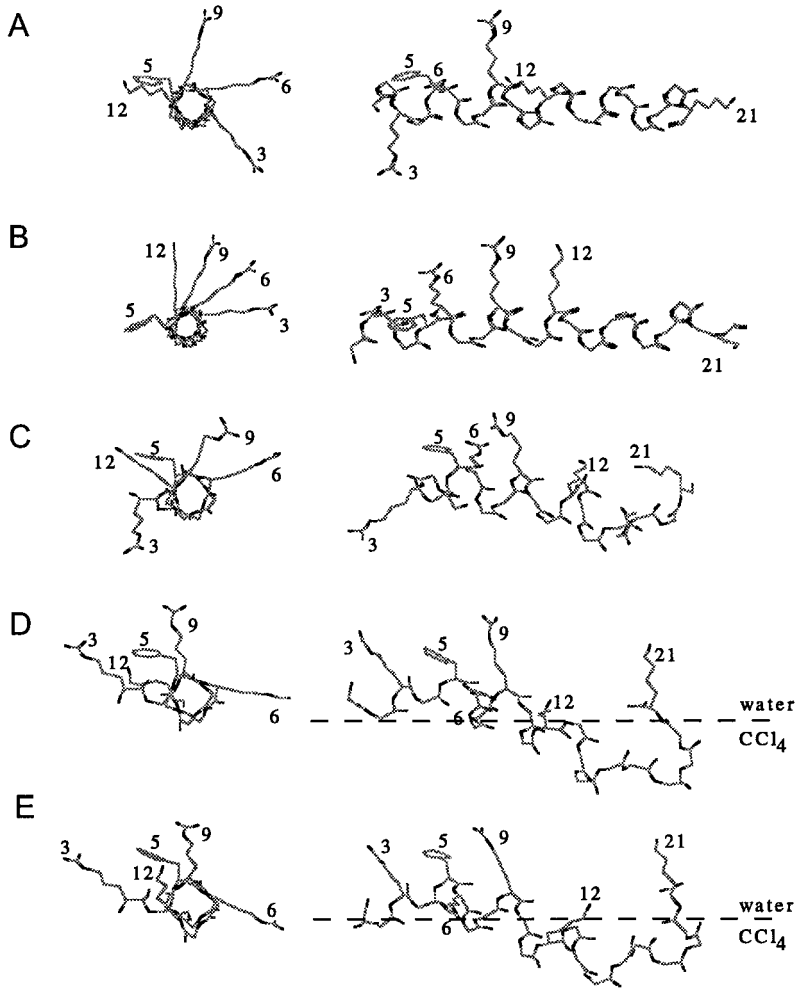

FIGURE 1 Structural models of the S4 peptide. The first column shows the orientation of the positively charged side chains of the region Arg-3–Lys-12 and Phe-5 when the peptide is viewed along the helix axis. The second column presents a side view of the backbone of the peptide and the heavy atoms of positively charged side chains. (*A*) α-helix, (*B*) 3_{10}-helix, (*C*) lowest-energy SA conformation based on the measured NOE constraints, (*D*) the structure after a 1.0-ns restrained simulation, and (*E*) structure after an additional 150-ps unrestrained simulation.

Kessler, 1994). The resulting model provides an illustrative summary of the experimental results and additional complementary information about the topological and conformational dynamics of peptide backbone, termini, and side chains in interfacial environments.

MATERIALS AND METHODS

Peptide synthesis and purification

The S4 peptide (first domain of the rat brain sodium channel) with the sequence ALRTFRVLRALKTISVIPGLK was prepared by solid-phase peptide synthesis using an ABI431 automatic peptide synthesizer and Fmoc/t-Bu chemistry (Atherton et al., 1981). At the doubly underlined position the Fmoc protected ^{15}N-labeled analog of alanine (Promochem, Wesel, Germany) was incorporated. For preparation of 0.25 mmol peptide a fourfold excess of protected amino acid (Applied Biosystems, Weiterstadt, Germany) was dissolved and activated for 6 min in a mixture of 2.1 g NMP and 2.2 g 0.45 M HBTU/HOBt in DMF. The coupling reaction to the HMP resin (0.96 mol/g, Applied Biosystems, Weiterstadt, Germany) was allowed to proceed for 30 min. For the 10 most N-terminal amino acids, coupling intervals were extended two to fourfold (^{15}N-Ala). Coupling steps were repeated for the ISVIP sequence and the three arginine residues. After removal of the Fmoc protecting group with 20% piperidine in NMP, the resin was thoroughly washed with NMP. The product was cleaved from the resin using a mixture of 0.75 g crystalline phenol, 0.25 ml EDT, 0.5 ml thioanisole, 0.5 ml H_2O, and 10 ml TFA, precipitated in ether and centrifuged. The high purity of the peptide was ensured by C18 reversed-phase HPLC and matrix-assisted laser desorption mass spectrometry. HPLC was performed using a gradient of 20–60% acetonitrile in water in the presence of 0.2% TFA at flow rates of 1 ml/min and a detection wave length of 220 nm.

High-resolution NMR spectroscopy

For solution NMR spectroscopy peptides were added to aqueous solutions of perdeuterated DPC (Promochem, Wesel, Germany) in 10 mM citrate-d5, pH 4–4.5 (Campro, Emmerich, Germany). Samples with detergent/peptide concentrations of 217 mM/3.9 mM and 322 mM/10.0 mM were used. In later experiments, TFE was added in a stepwise manner to yield final concentrations of organic solvent $\leq$30% (v/v).

The NMR spectra were acquired on a Bruker AMX 500 spectrometer at 300 K. For the resonance assignments and structural analysis, TOCSY (Griesinger et al., 1988) and NOESY spectra (Macura and Ernst, 1980) were acquired using data matrices of 2048 $\times$ 512 or 4096 $\times$ 512. Water suppression was achieved using the WATERGATE sequence with a gradient echo pulse sequence (Piotto et al., 1992). Alternatively, selective preirradiation or jump-return techniques were applied in some experiments (Plateau and Gueron, 1982). The applied mixing times were 100, 150, and 200 ms for the NOESY spectra and 60 ms and 100 ms for the TOCSY spectra. Before Fourier transform, phase-shifted sine-square apodisation functions and polynomial baseline corrections were applied. The processed matrix size was chosen between 2k $\times$ 1k and 4k $\times$ 4k. The classical methods were used to assign homonuclear NMR spectra and to calculate the NMR-derived conformations (Wüthrich, 1986). The selective ^{15}N label at alanine 10 provides a good starting point for the application of sequence-specific assignment strategies (Bechinger, 1997a). The hydrogen exchange rates of the amide protons of the S4 peptide were studied by dissolving a lyophilized peptide/DPC sample in D_2O and measuring TOCSY spectra immediately after sample preparation.

In order to obtain information about the peptide penetration into DPC micelles the spin-labeled fatty acids 5-DOXYL-stearate, 10-DOXYL-stearate, or 16-DOXYL-stearate were added to obtain final concentrations of 3.5–10 mM (Sigma-Aldrich, Steinheim, Germany). 5-DOXYL- and 16-DOXYL-stearate were added to the sample as a suspension in water. The amount of 10-DOXYL-stearate was measured from a methanolic solution. After removal of the organic solvent in high vacuum the appropriate amounts of DPC, peptide, and aqueous buffer were added. The effects of the spin labels were observed by comparing the peak volume intensities in TOCSY spectra of labeled with those of unlabeled samples.

Solid-state NMR spectroscopy

For solid-state NMR spectroscopy 15 mg of the S4 peptide (acetate salt) was dissolved in TFE/water and mixed with 320 mg phospholipid and dichloromethane (Avanti Polar Lipids, Birmingham, MA). The mixtures were slowly applied onto 35–40 thin cover glasses (11 $\times$ 22 mm), dried in air, and exposed to high vacuum over night. After the samples had been equilibrated in an atmosphere of 93% relative humidity, the glass plates were stacked on top of each other and sealed. Although at this vapor pressure bulk water is absent in the samples, most of the water association sites of lipid and peptide are saturated. The membrane stacks were introduced into the flat coil of a home-built solid-state NMR probe head (Bechinger and Opella, 1991) with the membrane normal of the uniaxially oriented bilayers oriented parallel to the magnetic field direction. The orientational degree of the phospholipid bilayers was routinely analyzed by proton-decoupled ^{31}P solid-state NMR spectroscopy (Bechinger et al., 1999b). Proton-decoupled ^{15}N solid-state NMR spectra were acquired on a wide-bore Bruker AMX400 spectrometer using a cross-polarization pulse sequence (Pines et al., 1973). Typical acquisition parameters were spin lock time 1.6 ms, recycle delay 3 s, ^{1}H B_1-field 1 mT, 254 data points, and spectral width 40 kHz. Signal averaging was performed overnight (25,000 transients). An exponential apodisation function (line-broadening 300) was applied before Fourier transformation. The chemical shifts were referenced with ^{15}N ammonium sulfate (27 ppm).

Computational methods

The distance restraints were obtained from NOESY spectra acquired with a 150-ms mixing time. All identified interresidual crosspeaks were integrated. The volume intensities were converted into distance constraints by comparing the peak intensities to the intraresidual crosspeaks of the Pro-18 side chain. To avoid too tight restraints the distances between amide protons were increased by 0.5 Å, the distances between all other atomic pairs by 1.0 Å. The conformational search was performed using the CVFF force field and the InsightII/Discover3 software package (Molecular Simulations Inc., San Diego, CA). The NOE constraints were included as an additional term in the force field by applying a simple harmonic function (force constant 100 kcal/(mol Å^2)), that added an energy penalty to the system when the distance in the model exceeded the restraint value. Several conformational search calculations were run. In each run a set of 100 conformations was created by means of an SA algorithm with slightly different restraint sets. In all cases, totally randomized initial conformations were used. The potential and restraint forces were gradually scaled to their full strength in 1000 K, after which the model was cooled to 300 K.

The conformation with the lowest potential energy was further studied in MD simulations. In these simulations the peptide was embedded into a solvent box consisting of a water and a tetrachloromethane phase (CCl_4). The parametrization of the box and the united atom model of CCl_4 were performed according to Moroder et al. (1993) and Guba and Kessler (1994). For water molecules the standard TIP3P model was used (Jorgensen et al., 1983). Periodic boundary conditions were applied in all dimensions of the 45 $\times$ 60 $\times$ 45 Å box. After removing the overlapping solvent molecules the system was optimized and simulated in the NVE ensemble. To enable application of 1-fs time steps, the high-frequency vibrations of hydrogens were removed with the RATTLE algorithm during the simulations (Anderson, 1983). Nonbonded interactions were cut off at 12 Å using a group-based method. Initially, the peptide was kept immobilized and the surrounding solvent was allowed to relax 1 ps. The next simulation step consisted of heating the whole system to 300 K for 6 ps, which was followed by a 30-ps equilibration period. During heating and equilibration, the NMR restraints were applied to the peptide. The actual

production simulation consisted of two periods: first the system was simulated for 1 ns with application of the NMR restraints, after which the simulation was continued for 150 ps without the restraints. The simulations were analyzed by studying the conformational fluctuations, the formation of hydrogen bonds, and their orientation with respect to the interface. In addition, two shorter simulations of 200 ps with different initial orientations of the peptide were performed.

RESULTS

In order to investigate the interactions of the S4 peptide with membrane interfaces, NOESY and TOCSY spectra of the peptide were recorded in the presence of DPC detergent micelles and initial structures of the peptide were calculated based on the measured geometrical NOE restraints (Fig. 1 *C*). Most of the close contacts resolved from our 100-ms and 150-ms NOESY spectra were also detected in the study of Doak et al. (1996). In our investigation two additional αN(*i, i* + 4) contacts between Phe-5 and Arg-9, Arg-6, and Ala-l0, and one αN(*i, i* + 3) contact between Ile-14 and Ile-17, are observed. However, our spectra do not resolve or show some αN(*i, i* + 3) and αN(*i, i* + 2) crosspeaks that have been reported previously; the latter have been attributed to spin diffusion (Doak et al., 1996). Differences in magnetic field strength (sensitivity and resolution), peptide-to-detergent-ratios, and mixing times may be responsible for these small differences. Comparison of the NOE connectivity pattern and the SA structures with those observed in TFE indicates an extension of the structured part of the peptide by a few residues toward the C-terminus in the presence of micellar interfaces (Figs. 1 *C* and 2).

When the NH chemical shift values measured in DPC micelles were compared to those observed in TFE/11% water (v/v) (Mulvey et al., 1989) a clear difference profile was observed (Fig. 2 *A, black bars*). Residues close to the unstructured ends of the peptide had up to 0.5 ppm larger chemical shifts than in TFE. In contrast, the shift values of the helical region Val-7–Ile-14 were up to 0.5 ppm smaller. Increased chemical shifts in the center of the peptide agree with an enhancement of the helical character in the core region of the peptide by TFE, but a weaker H-bonding interaction of the amide protons at the peptide termini upon replacement of water by the less basic TFE solvent (Nelson and Kallenbach, 1986; Sonnichsen et al., 1992). When TFE was added to S4/DPC samples in a stepwise manner the HN chemical shift values were detected to approach the ones observed in TFE (Fig. 2 *A, gray bars*). Only Leu-8, Arg-9, and Val-16 exhibit small shifts in the opposite direction. Despite the presence of high concentrations of DPC, TFE affects the chemical shifts throughout the sequence, suggesting that all amino acids interact with this solvent. Possible explanations are the partitioning of TFE and/or of the S4-peptide between the water and the micellar phase.

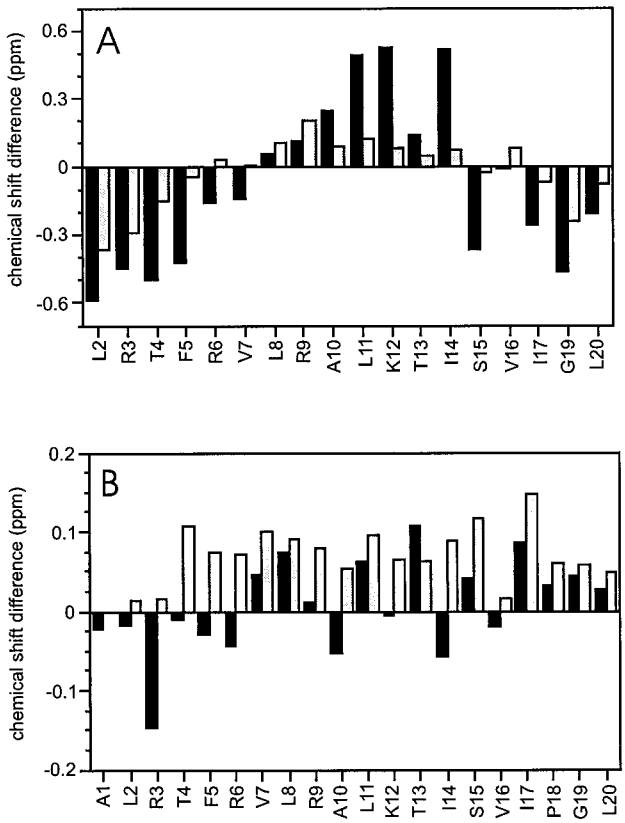

FIGURE 2 The differences between chemical shift values measured in TFE/11% water solutions (v/v) (Mulvey et al., 1989) and the values observed in aqueous solutions in the presence of DPC. (*A*) HN chemical shifts in TFE minus chemical shift in an aqueous DPC micellar solution (*black bars*), and after increasing the TFE concentration in the DPC micellar sample to 30% v/v (*gray bars*). (*B*) The differences of Hα chemical shifts observed in TFE and the water/DPC micellar environment (*black bars*), and after increasing the TFE concentration in the water/DPC sample to 30% v/v (*gray bars*). The values for Ala-1 and Lys-21 HN are not displayed since they are not observed in all cases.

Spin label experiments

The penetration and alignment of the peptide were studied by measuring TOCSY spectra from S4/DPC samples in the presence of 3.5–10 mM of 5-, 10-, or 16-DOXYL-stearate. Well-resolved crosspeaks were first integrated from a TOCSY spectrum of label-free sample and compared to the peak intensities observed in the presence of spin labels (Fig. 3). The DOXYL nitroxide radicals of these compounds are covalently attached to well-defined positions of the alkyl side chains of stearate; therefore, their effects on the NMR spectra of the peptide correlate with the average location and orientation of the peptide within the detergent micelle (Brown et al., 1981; Papavoine et al., 1995). In a first step the attenuation of each peak was evaluated. This result was consecutively transformed into an average attenuation value for each residue. It should be noted that the spin labels exhibit considerable flexibility within the micelle and lower the overall hydrophobicity of the fatty acyl chain. We therefore restrict ourselves to semiquantitative estimates of the spin label-induced decrease of the signal intensities. To a limited extent, signal intensities are also affected by spectral overlap, noise, the method of data processing, and the extension of the amino acid side chains. Clear differences in

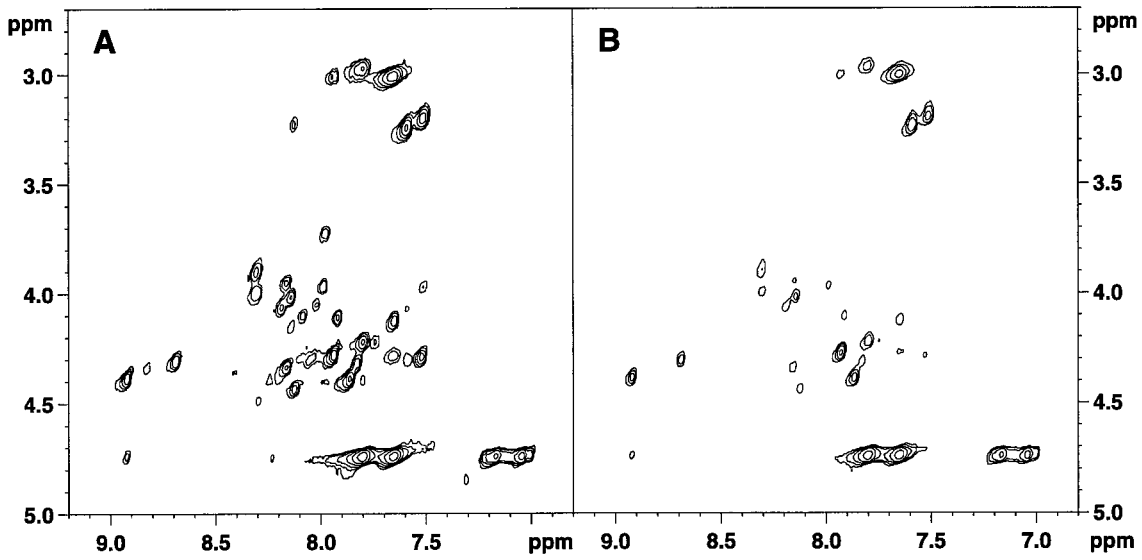

FIGURE 3 Fingerprint region of TOCSY NMR spectra of 3.7 mM S4 peptide in the presence of 285 mM perdeuterated DPC (*A*) in the absence and (*B*) in the presence of 3.5 mM 10-DOXYL-stearate. Mix time 100 ms, temperature 300 K.

the magnitude of the attenuation of different amino acids can be detected (Table 1).

The DOXYL spin label attached to the 5-position locates close to or within the interfacial region of the DPC micelle. In the presence of 10 mM 5-DOXYL-stearate most of the signals of the fingerprint region vanish; only weak signals remain from the β-protons of threonines and the α-protons of Arg-9, Ala-10, and Lys-12. The attenuation values obtained with this label are, therefore, mainly based to the remaining side chain crosspeaks (Table 1). In the presence of either 3.6 mM 10- or 16-DOXYL-stearate the crosspeaks of the fingerprint region were attenuated, but remained detectable. The widest distribution of the relative attenuation was obtained with 10-DOXYL-stearate. In this case a clear periodicity of 3–4 amino acids can be detected between Leu-2 and Ile-14 (Table 1). The side chains of the arginine and lysine residues exhibit the lowest degree of attenuation, indicating that these hydrophilic side chains are oriented furthest away from the micelle.

TABLE 1 The relative attenuation of TOCSY NMR crosspeak intensity by DOXYL spin labels

	Number of integrated peaks	5-DOXYL-stearate			10-DOXYL-stearate			16-DOXYL-stearate		
		L	M	S	L	M	S	L	M	S
Leu-2	3			S	L				M	
Arg-3	5		M			M			M	
Thr-4	5			S			S		M	
Phe-5	3			S		M			M	
Arg-6	3	L			L			L		
Val-7	7		M				S		M	
Leu-8	1		M			M		L		
Arg-9	6	L			L			L		
Ala-10	1	L			L			L		
Leu-11	1		M				S	L		
Lys-12	2		M		L			L		
Thr-13	3	L			L			L		
Ile-14	4		M				S		M	
Ser-15	3		M			M			M	
Val-16	5			S			S			S
Ile-17	3			S			S			S
Pro-18	13		M		L				M	
Gly-19	2		M		L				M	
Leu-20	1			S		M			M	
Lys-21	3			S		M			?	

Semiquantitative classification occurred according to L, low effect; M, moderate effect; S, strong effect.

No periodicity in the line-broadening could be detected when the paramagnetic cation Mn^{2+} was added to S4/DPC micelles in previous studies (Doak et al., 1996). We suspect that all residues of S4 are equally affected by this ion during times when the peptide resides in the aqueous solution. In contrast, the micelle-bound spin labels used in this work are only effective during the periods when S4 is associated with the DPC micelle.

Conformational search

A total of 31 sequential and 15 nonsequential connections were resolved from the NOESY spectra (Fig. 4). In vacuo, this set of geometrical restraints allows the peptide to fold into different irregular low-energy conformations. Long-range coulombic interactions are often overemphasized in the absence of polar solvents; therefore, the resulting peptide conformations bring the polar amino and carboxy termini close to each other. After excluding this kind of artificial conformations, the lowest energy structures shared a common helical backbone structure in the central part of the peptide.

To make the restraint set more complete and to reduce the conformational space, 16 additional restraints were added to the model to prevent some of such close contacts (<4 Å)

FIGURE 4 Graphical summary of resolved NOEs used for the simulated annealing calculations. The filled bars indicate the detected close contacts between amino acids. The open bars indicate the NOE peaks that were weak or unambiguously absent, and which were used as repulsive restraints during the conformational search.

that were unambiguously absent or weak in the NOESY spectra (Fig. 4). For both attractive and repulsive restraints a force constant of 100 kcal/(mol Å^2) was applied. With this modification, in a set of 100 SA-conformations, the 20 lowest-energy ones exhibit $\leq$0.1 Å violations of the geometrical restraints. All 100 structures shared α-helical conformations in the region Val-7 to Ala-10. In the regions 5–13 and 15–16, for each residue $>$50% of the phi/psi angular pairs are located in the helical region of the Ramachandran plot. The lowest-energy conformation is presented in Fig. 1 *C*.

MD simulations in a water/tetrachloromethane interface

The simulated annealing calculations were performed in vacuo. The conditions during the conformational search are, therefore, different from the actual micelle environment. In order to obtain a better estimate of the effects of the membrane interface, the lowest-energy conformation from the SA calculation was simulated in a membrane-mimicking environment. Because of limited computational resources, usage of an explicit lipid bilayer model was not considered. Instead, the peptide was placed into a periodic box with the dimensions 45 $\times$ 60 $\times$ 45 Å. One-half of the simulation box was filled with water and the remainder with CCl_4. Even though this biphasic environment provides only a rough estimate of the lipid bilayer interface, membrane-like effects had been successfully reproduced using this model in previous studies (Moroder et al., 1993; Guba and Kessler, 1994; Wymore and Wong, 1999a, b).

For the first simulation, the peptide was placed in the middle of the box along the interface in a manner that the hydrophobic face of the helix is oriented toward the CCl_4 phase. As a consequence, most of the charged side chains point toward the water phase. During the early phase of a 1.0-ns restrained simulation, the peptide quickly adapted to the environment, after which the peptide fluctuated around a single conformation that satisfied the geometrical restraints ($\leq$0.2 Å violations) and had only one undetected close contact of backbone protons (between Thr-13 Hα and Val-16 HN). In this equilibrium conformation, the region between Phe-5 and Ser-15 remained in an α-helical conformation, and α-helix-like hydrogen bonds were detected frequently (in over 30% of the conformations during the last 200 ps) between Thr-4 CO–Leu-8 HN, Phe-5–Arg-9, Val-7 CO–Leu-11 HN, and Ala-10 CO–Ile-14 HN (Fig. 1 *D*). Occasionally, 3_{10}-helix-like hydrogen bonds occurred as well, especially between Thr-4 CO and Val-7 HN. Throughout the helical region the conformation was stable, and standard deviations of phi and psi angles were $<$15° with the exception of fluctuations of the Thr-13 phi angle between $-$150° and $-$50°. The helix ended into a turn that was locked by a hydrogen bond between the Thr-13 carbonyl and the Val-16 amide. The amino acids following up to Pro-18 adopted a less regular structure characterized by a β-strand-like connection between Val-16–Ile-17 followed by a tight turn and a hydrogen bond between the Ile-17 carbonyl and the Gly-19 amide.

This conformation of the region Val-16–Gly-19 is probably a result of the change of the overall orientation of the peptide. Toward the end of the simulation the helical axis assumed a slightly tilted orientation with respect to the water-tetrachloromethane interface as the hydrophobic residues between Val-16 and Leu-20 moved deeper into the CCl_4 phase (Fig. 5). The β-strand-like conformation of Val-16 and Ile-17 allows both of these residues to turn away from the water phase. Other residues were also affected by the water/CCl_4 environment as the hydrophilic side chain of Arg-3, which would otherwise be exposed to the hydrophobic interior, bent toward the water phase (Fig. 1, *D* and *E*; Fig. 5).

The conformations resulting from the restrained MD simulation are in good agreement with the previous NMR

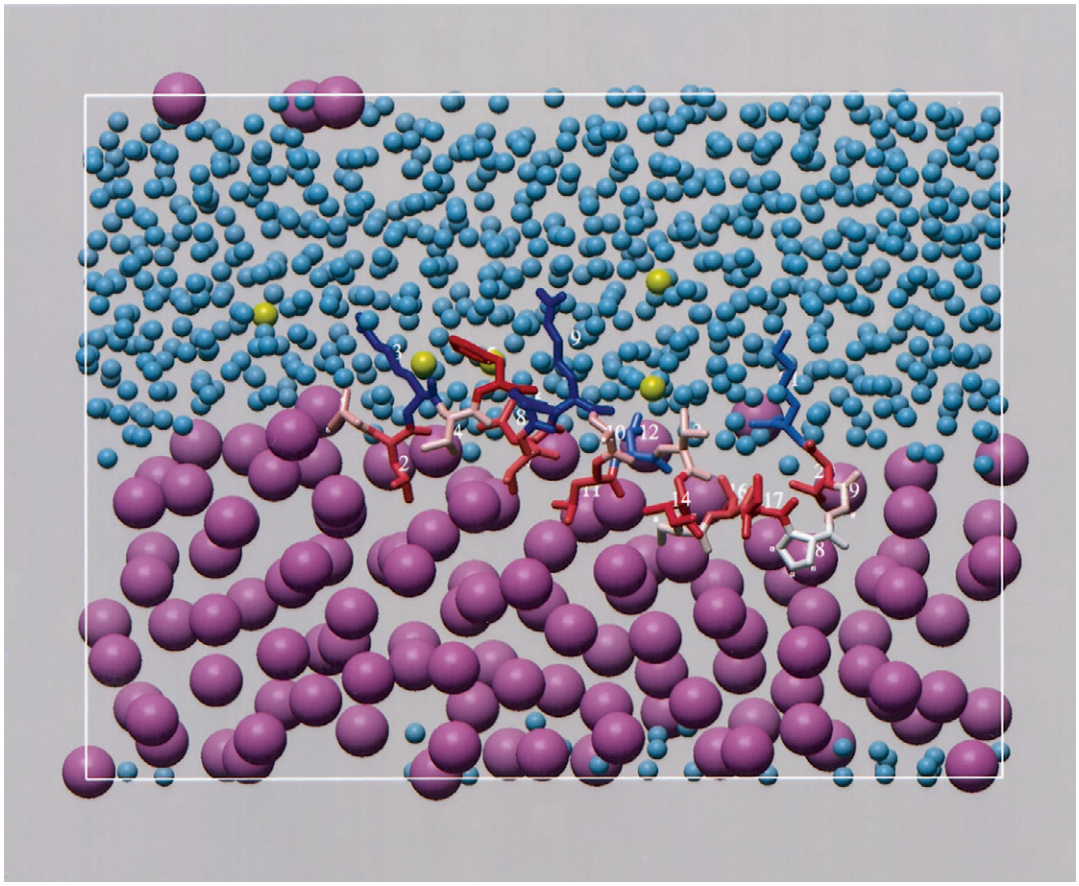

FIGURE 5 The S4 peptide conformation embedded in the tetrachloromethane/water two-phase box at the end of the restrained MD simulation. Only nonhydrogen atoms are displayed. Water molecules are shown in blue, tetrachloromethane molecules in magenta, and five Cl^- counterions in bright green. The peptide is color-coded in the following manner: charged side chains (*blue*), hydrophobic side chains (*red*), slightly hydrophobic side chains (*pink*), and proline 18 (*white*).

results of Doak et al. (1996). Some additional (*i, i*+3) and (*i, i*+4) crosspeaks were reported in their study, but could not be unambiguously resolved in our spectra. These additional contacts are also present in the simulated model. The only exceptions are three additional close contacts between Leu-2 Hα–Phe-5 HN, Arg-3 Hα-Arg-6 HN, and Arg-3 Hα–Arg-6 Hβ, all at the N-terminus of the peptide. In our model these residues remain in an extended conformation.

The simulation was compared to the spin label experiments by calculating the average penetration depths of the amino acids into the CCl_4 or the water phase during the last 200 ps of the simulation (Fig. 6). The values found for the residues located between Thr-4 and Ile-17 correlate well with the spin label experiments. Residues further toward the C-terminus, in particular Pro-18, are located deeper in the CCl_4 phase than the spin label experiments would suggest. These differences in the C-terminal region of the peptide, which occur when the experimental NMR results in the presence of spin labels are compared to the topology found during the simulations, are probably due to the high flexibility that is often inherent to loop regions and/or due to the bent surface geometry of the micelles that is not explicitly taken into consideration in the water/CCl_4 model system.

Removal of the NOE restraints causes some small changes to the conformation during the simulation in the two-phase box as the region around Lys-12–Thr-13 stopped fluctuating and assumed nonhelical conformations. Other regions of the peptide, however, remained in helical conformations (Fig. 1 *E*).

Additional 200-ps simulations were performed where the initial orientation of the peptide was changed by rotating the peptide by +90° or −90° around the helical axis. After a +90° rotation and embedding the peptide into the solvation box the Lys-12 side chain and the amino-terminus penetrate deeply into the hydrophobic phase. During the time course of the restrained simulation, the flexible amino terminus moved quickly into the aqueous phase. The central part of the peptide remained in helical conformations, but the peptide rotated around its long axis in order to allow the side chain of Lys-12 to get in contact with the water phase. At the same time the Val-16–Pro-18 region moved into the hydrophobic phase. As a result, the final orientation of the peptide resembled the orientation at the end of the previous 1-ns simulation.

When the peptide was rotated by −90°, Arg-6 was initially completely located within the CCl_4 phase. In this case,

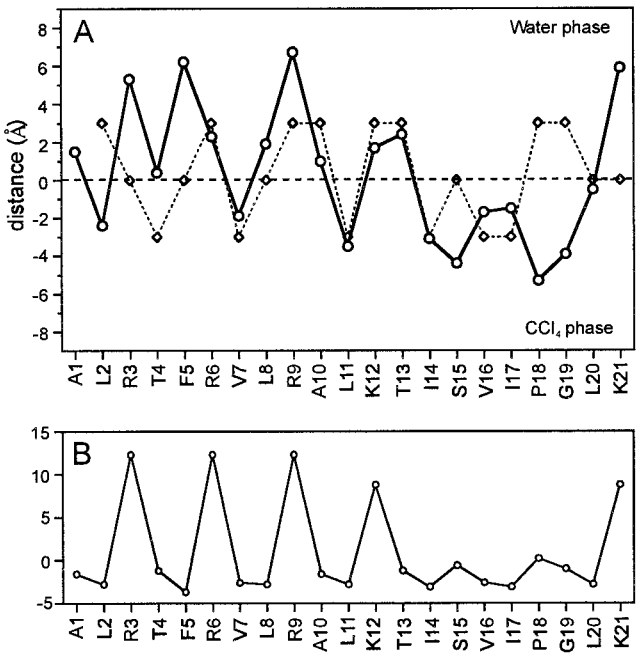

FIGURE 6 (*A*) Average location of hydrogens relative to the water/CCl_4 interface. The solid line displays values calculated from the simulation. These values were obtained by calculating average distance between the initial water/CCl_4 interfacial plane and each hydrogen during the last 200 ps of the restrained MD simulations. From these an average was calculated for each amino acid. The positive values correspond to locations in the water phase and the negative values to the CCl_4 phase. The dashed line refers to the 10-DOXYL-stearate experiments presented in Table 1. The used scaling (strong effect = −3 Å, moderate effect = 0 Å, low effect = 3 Å) is artificial and the values are presented only to make the comparison between experiment and simulation easier. (*B*) The hydrophobicity of the S4 amino acid side chains according to Engelman et al. (1986).

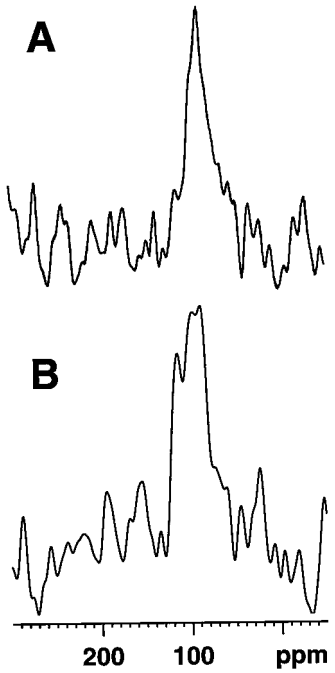

FIGURE 7 Proton-decoupled ^{15}N solid-state NMR spectra of 1.6 mol % S4 in oriented phospholipid bilayers. The peptide is labeled with ^{15}N at the Ala-10 position. The lipid bilayers are composed of (*A*) POPC, (*B*) POPC/POPS 1:1 mol/mol.

however, the hydrophilic side chain did not move toward the water phase. Instead, water molecules started to penetrate into the CCl_4 phase and a water-filled cavity formed around the Arg-6 side chain. The formation of water-filled cavities around charged residues has been observed previously in MD calculations (Berneche et al., 1998). In the simulation presented in the present paper, however, this behavior may be an artifact caused by the limited size of the periodic box. Most of the molecules forming the water cavity did not penetrate the CCl_4 phase directly through the interface in the center of the box where the peptide is located. Instead they left the box, crossed into the periodic image, and approached Arg-6 from the opposite side of the CCl_4 layer.

Solid-state NMR spectroscopy

Fig. 7 shows proton-decoupled ^{15}N solid-state NMR spectra of [^{15}N-Ala-10]-S4 reconstituted into oriented phospholipid bilayers. The ^{15}N chemical shift of helical peptides that are associated with uniaxially oriented lipid bilayers has been shown to be an indicator of the orientation of the helix axis with respect to the lipid bilayer. Whereas chemical shifts smaller than the isotropic value (120–130 ppm) correlate with helix orientations approximately parallel to the membrane surface, larger shifts are indicative of transmembrane alignments (Bechinger, 1996; Bechinger et al., 1991; 1996; 1999b). A chemical shift value of 89 ppm is observed for the alanine 10 position of the S4 segment, which is located in the central part of the α-helix (Fig. 7). This value is characteristic of an approximately in-plane orientation of the peptide. Fluctuations in the orientation of the Ala-10 ^{15}NH vector with respect to the magnetic field by $<10°$ are sufficient to explain the experimental linewidth in oriented proton-decoupled ^{15}N solid-state NMR spectra (Fig. 7). Reorientation of the alanine 10 residue, however, can be due to conformational and topological fluctuations of the helix, as well as undulations or misalignments of the bilayer surface.

In order to compare the solid-state NMR data with the results of the MD calculations, a protocol that has already been described in a previous publication was applied (Wray et al., 1999). During this analysis the static ^{15}N chemical shift values were calculated for all possible orientations of the S4 peptide with respect to the magnetic field direction. The peptide was taken in the lowest-energy helical conformation of the MD calculations (Figs. 1 *D*, 5). The experimental ^{15}N solid-state NMR data are in excellent agreement with the alignment of the peptide in the two-phase box when it is assumed that the CCl_4/water interface is representative of the phospholipid bilayer surface. Furthermore, the solid-state NMR data do also agree with the micellar surface location of the peptide found by spin label experiments.

DISCUSSION

Single-channel measurements indicate that in 0.5 M salt solutions the conductance of negatively charged phospholipid bilayers increases by 70, 300, or 500 pS due to the presence of S4 peptides (Tosteson et al., 1989). Whereas the level at 70 pS is permanently active, the latter two exhibit lifetimes of several milliseconds. A peptide where S4 is extended by the first 12 residues of the S4-S5 loop exhibits stepwise conductance increases of 8.4 pS in uncharged POPC-DOPE bilayers, or of 5.5 pS in negatively charged POPS-DOPE membranes (Brullemans et al., 1994). The Gaussian-like distribution of these transitions exhibits a half-width of 4–5 pS. In addition, larger conductance levels are observed at 15, 20, 40, and 80 pS. Model peptides, where the pattern of a charged amino acid at every third position has been maintained, $(XRL)_8$, exhibit conductances of 23 pS (X = A) or occasional fluctuations of 2 pS (X = V or L), respectively, when incorporated into negatively charged asolectin membranes (Iwata et al., 1994). In the presence of negatively charged phospholipid bilayers all of these peptides exhibit cation selectivity. This is in contrast to the large number of positive charges associated with the peptides and, therefore, suggests that the lipid headgroups form part of the conducting pore (Tosteson et al., 1989; Brullemans et al., 1994; Iwata et al., 1994).

The data presented in this and previous papers (Doak et al., 1996; Dempsey et al., 1998) indicate that the S4 peptide assumes helical conformations between residues 4 and 15 as well as a less regular structure up to residue 19 in membrane-like environments. The peptide resides in the interfacial regions of detergent micelles or lipid bilayers, with an orientation approximately perpendicular to the membrane normal. Spin label experiments indicate that the peptide intercalates into the bilayer and adopts an in-plane alignment. Molecular modeling studies show that a stable in-plane alignment and a reproducible orientation around the helix long axis are obtained when most of the hydrophobic residues of the helix are exposed to the membrane interior (Figs. 5, 6). At the same time, the arginine and lysine side chains are in contact with the water phase. Thus this orientation optimizes hydrophobic and electrostatic interactions between the environment and the peptide.

The formation of 3_{10} helical structures has been suggested for S4 and its related peptides, as this conformation results in a clear-cut separation of hydrophilic and hydrophobic residues (Iwata et al., 1994). Such a conformation allows for all hydrophobic side chains to be buried in the bilayer interior, whereas at the same time all charges point into the aqueous environment. Solution NMR spectroscopy of S4 in the presence of DPC micelles indicates, however, that the central part of the peptide occurs mostly in α-helical conformations. By NMR spectroscopic methods alone it is difficult to discern 3_{10} from α-helical structures (Gratias et al., 1998). Differentiating between these conformations solely from NOE patterns is even more demanding when helical conformations are in dynamical interchange. Molecular modeling and MD calculations, therefore, provide additional insights, and in the case of S4 embedded in a hydrophilic/hydrophobic interface does not show indications of extended 3_{10} H-bonding networks (this study). As pointed out previously a 3_{10} helical structure results in strong repulsive forces between the many positive charges accumulating on one face of the helix (Doak et al., 1996). Despite the exposure of a single hydrophobic phenylalanine residue to the aqueous environment (Fig. 5), the formation of central α-helical conformations with less regular structures toward the termini seems, therefore, energetically more favorable within the context of membrane interfaces. A gradient of the electric potential across the helix diameter could, however, favor the accumulation of residues of similar charge on one face of the helix, thereby inducing 3_{10} helical conformations oriented with the helix axis parallel to the bilayer surface (Iwata et al., 1994; Doak et al., 1996). The presence of less regular structures between residues 16 and 19 allows the hydrophobic residues valine 16 and leucine 17 to avoid penetration into the water phase. MD indicates that, although peptide side chains and termini cover a large conformational space, their average location within the hydrophobic/hydrophilic interface parallels the amino acid hydrophobicity (Fig. 6).

At first view these experimental findings of in-plane helix alignments seem in contrast to some of the common models for channel formation in which the peptides assume transmembrane orientations. These latter models are also in disagreement with the measured length of the helical portion of the S4 peptide, which is only ~12 amino acids long and insufficient to span the lipid bilayer completely. The in-plane alignment of the peptide corresponds to an energetically most favorable equilibrium state and is, therefore, detected by structural methods such as those described in this publication. It is, therefore, likely that the constantly active conductance state of 70 pS is caused by this in-plane configuration. The possibility exists, however, that a minor proportion of the peptides exist in transmembrane helical aggregates and causes some of the additional conductance states detected in single-channel electrophysiological recordings. In this case channel formation would require reorientation and extension of the helices during gating.

As the population of transmembrane channel-forming configurations may contain only a minor fraction of the total peptide, and therefore be too small to be detected by structural methods, a quantitative analysis of the energies of transition between the equilibrium in-plane configuration and the activated form of the channel is required to select among the suggested models. Although our understanding of the complex interactions within the lipid bilayers remains poor, estimates of the energies involved provide some valuable insight into the potential mechanisms of channel formation.

Whereas in a previous study the reorientation of helical peptides from an in-plane into a transmembrane alignment could be well-described by hydrophobic, electrostatic, and polar interactions (Bechinger, 1996), the aggregation of *n*

monomers to form a transmembrane helical bundle involves a more complicated set of interactions affecting to the total Gibbs free energy (ΔG). During the assembly process contributions arise from electrostatic repulsion of assembling the $5 \cdot n$ positive charges of the S4 fragments in the narrow channel opening (ΔG^{el}). In addition, entropic terms account for the loss of motional freedom for the assembling monomers (ΔG^{en}), and the van der Waals interactions between peptides and lipids are modified during this process (ΔG^{vW}).

In order to estimate ΔG^{el}, the energy of assembling 20 positively charged residues along the surface of a cylinder 30 Å long and 3 Å wide was calculated. When it is assumed that ~50% of the potential is screened by countercharges in the presence of 500 mM salt, the energy of tetramer formation (Brullemans et al., 1994) amounts to ~600 kJ/mol (Bechinger, 1997b). Similar numbers are obtained when the positively charged amino acids are converted into their corresponding uncharged bases at neutral pH. In this case the energy required is $\Delta G^{d} = n_i \cdot RT \cdot \ln r + 2.3RT\Sigma_i (pK_i - \text{pH})$, where i represents the amino acids that are discharged, n_i their total number, and $RT \ln r$ amounts to ~11.5 kJ/mol (Bechinger, 1997b). Equilibria between charged and uncharged forms of amino acid side chains may also be important when amino acid residues change their environment during the conformational transitions associated with voltage-gating of extended channel proteins.

Following the approach described by Jähnig (1983) an estimate of the loss of energy due to peptide immobilization during tetramer formation (ΔG^{en}) yields ~200 kJ/mol. Although modeling calculations indicate that the van der Waals interactions of forming 20-residue-peptide dimers amounts to −100 to −160 kJ/mol in vacuo (Pullman, 1988; Breed et al., 1995), the net change in van der Waals energy when peptide-lipid interactions are replaced by peptide-peptide and lipid-lipid interactions is much more difficult to determine.

Additional energy contributions that are favorable to reorientation arise when a transmembrane electric potential pulls the helix dipoles inside the membrane ($\Delta G^{\Psi} \leq n \cdot 10$ kJ/mol (Bechinger, 1997b)). As the C-terminal lysines are more easily discharged when compared to N-terminal arginines, the dipole moment along the long axis of the peptide is potentially enhanced. The sum of other energy contributions such as the lipophobic effect and van der Waals interactions between the lipid side chains is comparatively small (Jähnig, 1981).

To explain the high frequency of openings observed in single-channel measurements (Tosteson et al., 1989; Brullemans et al., 1994) the total energy ΔG of tetramer formation should be close to zero. The above considerations indicate that the unfavorable electrostatic and entropic terms (≈800 kJ/mol) would have to be compensated by other strong interactions (ΔG^{vW}, etc.) which, in addition to ΔG^{Ψ}, favor the formation of transmembrane helical peptide aggregates.

Alternatively, models for channel formation in which the lipids are part of the channel-forming structure have been suggested (reviewed in Bechinger, 1997b). In one of these models it is proposed that in-plane helices destabilize the packing of the membrane. Lateral diffusion along the bilayer surface results in fluctuations of the local peptide density. When two or more of these peptides approach each other, areas of membrane instability overlap and transient bilayer openings occur. This latter model is in agreement with experimental findings including the cooperativity of channel formation (Tosteson et al., 1989; Brullemans et al., 1994), the stable in-plane orientation of peptides (this study), the modest cation selectivity, and the experimentally observed variability of the conductance increases (Tosteson et al., 1989; Brullemans et al., 1994; Iwata et al., 1994). Furthermore, the average distance between chromophore-labeled S4 monomers and their location within the membrane have been shown to be unaffected by transmembrane diffusion potentials (Rapaport et al., 1992). The apparent gating charges of these conducting units, calculated from the current-voltage relationships, range between 1 and 3 (Tosteson et al., 1989; Brullemans et al., 1994). These gating charges may be due to conformational alterations such as an increase in helicity, α- to 3_{10}-helix transitions, and changes in bilayer penetration and membrane association (Stankowski et al., 1988; Sigworth, 1992), or a combination of these effects.

Electrophysiological recordings indicate that S4 channel formation occurs in charged and uncharged lipid membranes; the size of the channels and the probability of openings are, however, dependent on the lipids used during the experimental measurements (Brullemans et al., 1994). In addition, S4-induced permeation of membranes to calcein (MW 623) requires the presence of negatively charged phospholipids (Rapaport et al., 1992). Whereas some functional properties of S4 thus depend on lipid composition, the ^{15}N solid-state NMR spectra of the peptide in oriented membranes do not reveal major conformational or topological differences when S4 is associated with either PC or mixed PS/PC bilayers (Fig. 7). The experimentally determined decrease in intermolecular distance between S4 peptides upon addition of negatively charged phospholipids (Rapaport et al., 1992) suggests, however, that in-plane phase separation of regions rich in negatively charged lipids and cationic peptides occurs (Wang et al., 1993; Welti and Glaser, 1994). At high peptide concentrations the presence of acidic phospholipids has been proposed to result in self-association of in-plane peptides in a "carpet-like" manner (Rapaport et al., 1992; Gazit et al., 1995). The possibility therefore exists that without major changes in the conformation or topology of the peptide, the size and frequency of lipid-mediated channels are regulated by the physical characteristics of membrane lipids. In addition, phospholipids vary in their fatty acyl chain packing characteristics, their phase diagrams and, as a consequence, also in their sensitivity with respect to interacting substances.

Channel formation has also been observed for other positively charged amphipathic peptides, including the antibiotics magainins (Cruciani et al., 1992; Duclohier et al., 1989), cecropins (Christensen et al., 1988), melittin (Tosteson and Tosteson, 1981; Hanke et al., 1983; Tosteson et al., 1987), mastoparan (Mellor and Sansom, 1990), or short synthetic polypeptides (Lear et al., 1988; Balaram et al., 1992). Interestingly, detergents or vesicle suspensions also exhibit channel-like properties when added to black lipid membranes (Schlieper and De Robertis, 1977; Alder et al., 1991; Woodbury, 1989). Related mechanisms of lipid-mediated pore formation may apply, in particular when considering that a wide variety of complementary methods indicate stable in-plane alignments for both S4 (this study) and magainin antibiotic peptides (Bechinger, 1997b).

We are grateful to Ingrid Neidhart and Christoph Eckerskorn for the synthesis of the S4 peptide and its mass spectrometric analysis. We are much indebted to Horst Kessler and his co-workers from whom we received the program and the force field to set up the two-phase box. The conformational search and MD simulations were performed using the SGI Power Onyx computer of CSC-Center for Scientific Computing (The Finnish national supercomputing center, Espoo, Finland).

REFERENCES

Alder, G. M., W. M. Arnold, C. L. Bashford, A. F. Drake, C. A. Pasternak, and U. Zimmermann. 1991. Divalent cation-sensitive pores formed by natural and synthetic melittin and by triton X-100. *Biochim. Biophys. Acta*. 1061:111–120.

Anderson, H. C. 1983. RATTLE: a "velocity" version of the Shake algorithm for molecular dynamics calculations. *J. Comp. Phys.* 52: 24–34.

Atherton, E., C. J. Logan, and R. C. Sheppart. 1981. Peptide synthesis: Part 2. Procedures for solid-phase synthesis using N^a-fluorenyllmethoxycarbonylamino-acids on polyamide supports. Synthesis of substance P and of acyl carrier proteins 65–74 decapeptide. *J. Chem. Soc. Perkin Trans. I*. 538–546.

Balaram, P., K. Krishna, M. Sukumar, I. R. Mellor, and M. S. Sansom. 1992. The properties of ion channels formed by zervamicins. *Eur. Biophys. J.* 21:117–128.

Bechinger, B. 1996. Towards membrane protein design: pH dependent topology of histidine-containing polypeptides. *J. Mol. Biol.* 263: 768–775.

Bechinger, B. 1997a. Structure and dynamics of the M13 coat protein signal sequence in membranes. *Proteins: Struct., Funct., Genet.* 27: 481–492.

Bechinger, B. 1997b. Structure and functions of channel-forming polypeptides: magainins, cecropins, melittin and alamethicin. *J. Membr. Biol.* 156:197–211.

Bechinger, B., L. M. Gierasch, M. Montal, M. Zasloff, and S. J. Opella. 1996. Orientations of helical peptides in membrane bilayers by solid-state NMR spectroscopy. *Solid State Nucl. Magn. Reson.* 7:185–192.

Bechinger, B., Y. Kim, L. E. Chirlian, J. Gesell, J.-M. Neumann, M. Montal, J. Tomich, M. Zasloff, and S. J. Opella. 1991. Orientations of amphipathic helical peptides in membrane bilayers determined by solid-state NMR spectroscopy. *J. Biomol. NMR*. 1:167–173.

Bechinger, B., R. Kinder, M. Helmle, T. B. Vogt, U. Harzer, and S. Schinzel. 1999b. Peptide structural analysis by solid-state NMR spectroscopy. *Biopolymers.* In press.

Bechinger, B., and S. J. Opella. 1991. Flat-coil probe for NMR spectroscopy of oriented membrane samples. *J. Magn. Reson.* 95:585–588.

Bechinger, B., J. M. Ruysschaert, and E. Goormaghtigh. 1999a. Membrane helix orientation from linear dichroism of infrared attenuated total reflection spectra. *Biophys. J.* 76:552–563.

Ben-Efraim, I., and Y. Shai. 1996. Secondary structure, membrane localization, and coassembly within phospholipid membranes of synthetic segments derived from the N- and C-termini regions of the ROMK1 K+ channel. *Protein Sci.* 5:2287–2297.

Berneche, S., M. Nina, and B. Roux. 1998. Molecular dynamics simulation of melittin in a dimyristoylphosphatidylcholine bilayer membrane. *Biophys. J.* 75:1603–1618.

Betz, H. 1990. Homology and analogy in transmembrane channel design: lessons from synaptic membrane proteins. *Biochemistry*. 29:3591–3599.

Biggin, P. C., J. Breed, H. S. Son, and M. S. P. Sansom. 1997. Simulation studies of alamethicin-bilayer interactions. *Biophys. J.* 72:627–636.

Breed, J., I. D. Kerr, R. Sankararamakrishnan, and M. S. Sansom. 1995. Packing interactions of Aib-containing helices: molecular modeling of parallel dimers of simple hydrophobic helices and of alamethicin. *Biopolymers*. 35:639–655.

Brown, L. R., C. Bosch, and K. Wüthrich. 1981. Location and orientation relative to the micelle surface for glucagon in mixed micelles with dodecylphosphocholine; EPR and NMR studies. *Biochim. Biophys. Acta*. 642:296–312.

Brullemans, M., O. Helluin, J. Y. Dugast, G. Molle, and H. Duclohier. 1994. Implication of segment S45 in the permeation pathway of voltage-dependent sodium channels. *Eur. Biophys. J.* 23:39–49.

Chen, L. Q., V. Santarelli, R. Horn, and R. G. Kallen. 1996. A unique role for the S4 segment of domain 4 in the inactivation of sodium channels. *J. Gen. Physiol.* 108:549–556.

Christensen, B., J. Fink, R. B. Merrifield, and D. Mauzerall. 1988. Channel-forming properties of cecropins and related model compounds incorporated into planar lipid membranes. *Proc. Natl. Acad. Sci. USA*. 85:5072–5076.

Cruciani, R. A., J. L. Barker, G. Raghunathan, H. R. Guy, M. Zasloff, and E. F. Stanley. 1992. Magainin 2, a natural antibiotic from frog skin, forms ion channels in lipid bilayer membranes. *Eur. J. Pharmacol.* 226:287–296.

Dempsey, C. E., R. B. Sessions, A. Halsall, J. Takei, N. Gibbs, and M. T. Young. 1998. Helical structure and dynamics in membrane polypeptides. *Biochem. Soc. Trans.* 26:444–450.

Doak, D. G., D. Mulvey, K. Kawaguchi, J. Villalain, and I. D. Campbell. 1996. Structural studies of synthetic peptides dissected from the voltage-gated sodium channel. *J. Mol. Biol.* 258:672–687.

Ducarme, P., M. Rahman, and R. Brasseur. 1998. IMPALA: a simple restraint field to simulate the biological membrane in molecular structure studies. *Proteins*. 30:357–371.

Duclohier, H., G. Molle, and G. Spach. 1989. Antimicrobial peptide magainin I from *Xenopus* skin forms anion-permeable channels in planar lipid bilayers. *Biophys. J.* 56:1017–1021.

Engelman, D. M., T. A. Steitz, and A. Goldman. 1986. Identifying nonpolar transbilayer helices in amino acid sequences of membrane proteins. *Annu. Rev. Biophys. Biophys. Chem.* 15:321–353.

Gazit, E., A. Boman, H. G. Boman, and Y. Shai. 1995. Interaction of the mammalian antibacterial peptide cecropin P1 with phospholipid vesicles. *Biochemistry*. 34:11479–11488.

Gratias, R., R. Konat, H. Kessler, M. Crisma, G. Valle, A. Polese, F. Formaggio, C. Toniolo, Q. B. Broxterman, and J. Kamphuis. 1998. First step toward the quantitative identification of peptide 3_{10}-helix conformation with NMR spectroscopy: NMR and x-ray diffraction structural analysis of fully developed 3_{10}-helical peptide standard. *J. Am. Chem. Soc.* 120:4763–4770.

Grice, A. L., I. D. Kerr, and M. S. P. Sansom. 1997. Ion channels formed by HIV-1 Vpu: a modelling and simulation study. *FEBS Lett.* 405: 299–304.

Griesinger, C., G. Otting, K. Wüthrich, and R. R. Ernst. 1988. Clean TOCSY for ^{1}H spin system identification in macromolecules. *J. Am. Chem. Soc.* 110:7870–7872.

Guba, W., and H. Kessler. 1994. A novel computational mimetic of biological membranes in molecular dynamics simulations. *J. Phys. Chem.* 98:23–27.

Hanke, W., C. Methfessel, H. U. Wilmsen, E. Katz, G. Jung, and G. Boheim. 1983. Melittin and a chemically modified trichotoxin form alamethicin-type multi-state pores. *Biochim. Biophys. Acta*. 727: 108–114.

Haris, P. I., B. Ramesh, S. Brazier, and D. Chapman. 1994. The conformational analysis of a synthetic S4 peptide corresponding to a voltage-gated potassium ion channel protein. *FEBS Lett.* 349:371–374.

Iwata, T., S. Lee, O. Oishi, H. Aoyagi, M. Ohno, K. Anzai, Y. Kirino, and G. Sugihara. 1994. Design and synthesis of amphipathic 3_{10}-helical peptides and their interactions with phospholipid bilayers and ion channel formation. *J. Mol. Biol.* 269:4928–4933.

Jähnig, F. 1981. Critical effects from lipid-protein interaction in membranes. I. Theoretical description. *Biophys. J.* 36:329–345.

Jähnig, F. 1983. Thermodynamics and kinetics of protein incorporation into membranes. *Proc. Natl. Acad. Sci. USA*. 80:3691–3695.

Jorgensen, W. L., J. D. Chandraeskar, J. D. Maruda, R. W. Impey, and M. L. Klein. 1983. Comparison of simple potential functions for simulating liquid water. *J. Chem. Phys.* 79:926–935.

Kontis, K. J., A. Rounaghi, and A. L. Goldin. 1997. Sodium channel activation gating is affected by substitutions of voltage sensor positive charges in all four domains. *J. Gen. Physiol.* 110:391–401.

Kra-Oz, Z., G. Spira, Y. Palti, and H. Meiri. 1992. Involvement of different S4 parts in the voltage dependency of Na channel gating. *J. Membr. Biol.* 129:189–198.

Lear, J. D., Z. R. Wasserman, and W. F. DeGrado. 1988. Synthetic amphiphilic peptide models for protein ion channels. *Science*. 240: 1177–1181.

Logothetis, D. E., S. Movahedi, C. Satler, K. Lindpaintner, and B. Nadal-Ginard. 1992. Incremental reductions of positive charge within the S4 region of a voltage-gated K+ channel result in corresponding decreases in gating charge. *Neuron*. 8:531–540.

Macura, S., and R. R. Ernst. 1980. Elucidation of cross relaxation in liquids by two-dimensional NMR spectroscopy. *Mol. Phys.* 41:95.

Mannuzzu, L. M., M. M. Moronne, and E. Y. Isacoff. 1996. Direct physical measure of conformational rearrangement underlying potassium channel gating. *Science*. 271:213–216.

Mellor, I. R., and M. S. P. Sansom. 1990. Ion-channel properties of mastoparan, a 14-residue peptide from wasp venom, and of MP3, a 12-residue analogue. *Proc. R. Soc. Lond. B*. 239:383–400.

Milik, M., and J. Skolnick. 1993. Insertion of peptide chains into lipid membranes: an off-lattice Monte Carlo dynamics model. *Proteins*. 15: 10–25.

Montal, M. 1990. Molecular anatomy and molecular design of channel proteins. *FASEB J.* 4:2623–2635.

Moroder, L., R. Romano, W. Guba, D. F. Mierke, H. Kessler, C. Delporte, J. Winand, and J. Christophe. 1993. New evidence for a membrane-bound pathway in hormone receptor binding. *Biochemistry*. 32: 13551–13559.

Mulvey, D., G. F. King, R. M. Cooke, D. G. Doak, T. S. Harvey, and I. D. Campbell. 1989. High resolution 1H NMR study of the solution structure of the S4 segment of the sodium channel protein. *FEBS Lett.* 257:113–117.

Nelson, J. W., and N. R. Kallenbach. 1986. Stabilization of the ribonuclease S-peptide alpha-helix by trifluoroethanol. *Proteins*. 1:211–217.

Noda, M., S. Shimizu, T. Tanabe, T. Takai, T. Kayano, T. Ikeda, H. Takahashi, H. Nakayama, Y. Kanaoka, N. Minamino, K. Kangawa, H. Matsuo, M. A. Raftery, T. Hirose, S. Inayama, H. Hayashida, T. Miyata, and S. Numa. 1984. Primary structure of *Electrophorus electricus* sodium channel deduced from cDNA sequence. *Nature*. 312:121–127.

Oblatt-Montal, M., L. K. Bühler, T. Iwamoto, J. M. Tomich, and M. Montal. 1993. Synthetic peptides and four-helix bundle proteins as model systems for the pore-forming structure of channel proteins. *J. Biol. Chem.* 268:14601–14607.

Papavoine, C. H., J. M. Aelen, R. N. Konings, C. W. Hilbers, and F. J. Van de Ven. 1995. NMR studies of the major coat protein of bacteriophage M13. Structural information of gVIIIp in dodecylphosphocholine micelles. *Eur. J. Biochem.* 232:490–500.

Pellegrini, M., A. Bisello, M. Rosenblatt, M. Chorev, and D. F. Mierke. 1998. Binding domain of human parathyroid hormone receptor: from conformation to function. *Biochemistry*. 37:12737–12743.

Pines, A., M. G. Gibby, and J. S. Waugh. 1973. Proton-enhanced NMR of dilute spins in solids. *J. Chem. Phys.* 59:569–590.

Piotto, M., V. Saudek, and V. Sklenar. 1992. Gradient-tailored excitation for single-quantum NMR spectroscopy of aqueous solutions. *J. Biomol. NMR*. 2:661–665.

Plateau, P., and M. Gueron. 1982. Exchangeable proton NMR without base-line distortion using new strong pulse sequences. *J. Am. Chem. Soc.* 104:7310–7311.

Pullman, A. 1988. Theoretical studies on the formation and properties of bundles of alpha-helices and their aptitude to form ion-channels. *Prog. Clin. Biol. Res.* 273:113–120.

Rapaport, D., M. Danin, E. Gazit, and Y. Shai. 1992. Membrane interactions of the sodium channel S4 segment and its fluorescently-labeled analogues. *Biochemistry*. 31:8868–8875.

Schlieper, P., and E. De Robertis. 1977. Triton X-100 as a channel-forming substance in artificial lipid bilayer membranes. *Arch. Biochem. Biophys.* 184:204–208.

Sigworth, F. J. 1992. Voltage gating of ion channels. *Q. Rev. Biophys.* 27:1–40.

Sonnichsen, F. D., J. E. Van Eyk, R. S. Hodges, and B. D. Sykes. 1992. Effect of trifluoroethanol on protein secondary structure: an NMR and CD study using a synthetic actin peptide. *Biochemistry*. 31:8790–8798.

Stankowski, S., U. D. Schwarz, and G. Schwarz. 1988. Voltage-dependent pore activity of the peptide alamethicin correlated with incorporation in the membrane: salt and cholesterol effects. *Biochim. Biophys. Acta*. 941:11–18.

Stühmer, W. 1991. Structure-function studies of voltage-gated ion channels. *Annu. Rev. Biophys. Biophys. Chem.* 20:65–78.

Stühmer, W., F. Conti, H. Suzuki, X. D. Wang, M. Noda, N. Yahagi, H. Kubo, and S. Numa. 1989. Structural parts involved in activation and inactivation of the sodium channel. *Nature*. 339:597–603.

Tosteson, M. T., D. S. Auld, and D. C. Tosteson. 1989. Voltage-gated channels formed in lipid bilayers by a positively charged segment of the Na-channel polypeptide. *Proc. Natl. Acad. Sci. USA*. 86:707–710.

Tosteson, M. T., J. J. Levy, L. H. Caporale, M. Rosenblatt, and D. C. Tosteson. 1987. Solid-phase synthesis of melittin: purification and functional characterization. *Biochemistry*. 26:6627–6631.

Tosteson, M. T., and D. C. Tosteson. 1981. The sting. Melittin forms channels in lipid bilayers. *Biophys. J.* 36:109–116.

Vogt, T. C. B., and B. Bechinger. 1999. The interactions of histidine-containing amphipathic helical peptide antibiotics with lipid bilayers: the effects of charges and pH. *J. Biol. Chem.* In press.

Wang, F., G. H. Naisbitt, L. P. Vernon, and M. Glaser. 1993. Pyrularia thionin binding to and the role of tryptophan-8 in the enhancement of phosphatidylserine domains in erythrocyte membranes. *Biochemistry*. 32:12283–12289.

Welti, R., and M. Glaser. 1994. Lipid domains in model and biological membranes. *Chem. Phys. Lipids*. 73:121–137.

Woodbury, D. J. 1989. Pure lipid vesicles can induce channel-like conductances in planar bilayers. *J. Membr. Biol.* 109:145–150.

Wray, V., R. Kinder, T. Federau, P. Henklein, B. Bechinger, and U. Schubert. 1999. Solution structure and orientation of the transmembrane anchor domain of the HIV-1 encoded virus protein U (Vpu) by high-resolution and solid-state NMR spectroscopy. *Biochemistry*. 38: 5272–5282.

Wüthrich, K. 1986. NMR of Proteins and Nucleic Acids. John Wiley and Sons, New York.

Wymore, T., and T. C. Wong. 1999a. Molecular dynamics study of substance P peptides in a biphasic membrane mimic. *Biophys. J.* 76: 1199–1212.

Wymore, T., and T. C. Wong. 1999b. Molecular dynamics study of substance P peptides in a sodium dodecyl sulfate micelle. *Biophys. J.* 76:1213–1227.

Yang, N., A. L. George, Jr., and R. Horn. 1996. Molecular basis of charge movement in voltage-gated sodium channels. *Neuron*. 16:113–122.